Bioorganic Chemistry 91 (2019) 103168

Contents lists available at ScienceDirect

Bioorganic Chemistry

journal homepage: www.elsevier.com/locate/bioorg

Strategy and validation of a structure-based method for the discovery of selective inhibitors of PAK isoforms and the evaluation of their anti-cancer activity

Pei-Lu Song[a], Gang Wang[c], Yuan Su[a], Han-Xun Wang[a], Jian Wang[a,*], Feng Li[b,*], Mao-Sheng Cheng[a,*]

[a] Key Laboratory of Structure-Based Drug Design & Discovery of Ministry of Education, Shenyang Pharmaceutical University, Shenyang 110016, China
[b] Department of Cell Biology, Key Laboratory of Cell Biology, Ministry of Public Health, and Key Laboratory of Medical Cell Biology, Ministry of Education, China Medical University, Shenyang 110001, China
[c] Center for Drug Evaluation, National Medical Products Administration, Beijing 100022, China

ARTICLE INFO

Keywords:
Virtual screening
Molecular dynamics simulation
Biotin-avidin system
PAK4 inhibitor

ABSTRACT

p21 activated kinase 4 (PAK4), which belongs to the serine/threonine (Ser/Thr) protein kinase family, is a representative member of the PAK family and plays a significant role in multiple processes associated with cancer development. In this study, structure-based virtual screening was performed to discover novel and selective small molecule scaffolds, and a 6-hydroxy-2-mercapto-3-phenylpyrimidin-4(3*H*)-one-based compound (SPU-106, 14#) was identified as an effective PAK4 inhibitor. By combining both a molecular docking study and molecular dynamics (MD) simulation strategies, the binding mode was determined in the PAK4 site. The SPU-106 compound could efficiently and selectively bind to the PAK4 kinase domain at an IC_{50} of 21.36 μM according to the kinase analysis. The designed molecular probe demonstrated that SPU-106 binds to the kinase domain in the C-terminus of PAK4. Further investigation revealed that the SPU-106 had a strong inhibitory effect on the invasion of SGC7901 cells but without any cytotoxicity. The western blot analysis indicated that the compound potently inhibited the PAK4/LIMK1/cofilin and PAK4/SCG10 signaling pathways. Thus, our work shows the successful application of computational strategies for the discovery of selective hits, and SPU-106 may be an effective PAK4 inhibitor for further development as an antitumor agent.

1. Introduction

p21-activated kinases (PAKs) belong to a family of serine/threonine (Ser/Thr) protein kinases that are broadly classified into two groups based on structural characteristics and regulatory mechanisms: PAK1, 2, and 3 (group I) and PAK4, 5, and 6 (group II) [1,2]. Of all of the PAKs, PAK4 is the most extensively studied of the group II PAK members and is positioned at the nexus of multiple signaling pathways [3]. PAK4 is an important downstream mediator of Cdc42. Many studies have demonstrated that the activation of PAK4 could protect cells from apoptosis, promote cell migration, and inhibit cell adhesion and anchorage-independent growth [4]. The broad upregulation of PAK4 expression has been observed in most cancer cell lines [5–7]. In athymic mice, the overexpression of PAK4 leads to tumor formation and the reduction of the inhibition of tumorigenesis by PAK4 [6]. The rationale for targeting PAK4 is based on its involvement in signal transduction hubs and regulatory functioning in physiology and pathological conditions [4]. However, a recent study demonstrated that the inhibition of PAK2 is associated with increased acute cardiovascular toxicity, which may be reinforced by PAK1 inhibition [8]. Thus, the development of a selective and effective PAK4 inhibitor is desirable for reducing potential adverse side effects and may serve as a helpful tool for improving our understanding of PAK4 cellular functions.

Over the past 20 years, several inhibitors with different levels of activity and selectivity have been developed for various PAK isoforms. Among them, only two PAK4 inhibitors have entered phase I clinical trials: PF3758309 (NCT00932126) and KPT-9274 (NCT02702492). PF3750309 is actually a 'Pan-PAK' inhibitor, although it is defined as a PAK4 inhibitor [9]. However, it was desired to avoid the inhibition of group I PAKs. Unfortunately, these clinical trials were discontinued due to low oral bioavailability, a lack of tumor responses and serious adverse events [10]. KPT-9274, which is known as a PAK4 allosteric

* Corresponding authors.
E-mail addresses: jianwang@syphu.edu.cn (J. Wang), fli@mail.cmu.edu.cn (F. Li), mscheng@syphu.edu.cn (M.-S. Cheng).

https://doi.org/10.1016/j.bioorg.2019.103168
Received 4 July 2019; Received in revised form 29 July 2019; Accepted 29 July 2019
Available online 30 July 2019
0045-2068/

inhibitor, is a PAK4 and NAMPT dual-target inhibitor for the treatment of solid malignancies or non-Hodgkin's lymphoma (NHL) [11]. It utilizes a novel mechanism of protein kinase inactivation that involves the destabilization of PAK4 rather than the direct inhibition of the kinase activity [12]. Although the compound has entered clinical trials, its acting site and binding mode with PAK4 protein are still unclear, which indicates that it would be very difficult to base the rational design of drugs on this research. Therefore, there is an urgent need to design compounds that act directly against the PAK4 kinase domain, even if it is very difficult to achieve selectivity.

Our research group has had a keen interest in the discovery of potential and selective PAK4 inhibitors as new therapeutic agents for cancers over the past ten years [3,13–21]. Great progress has been achieved in multiple areas involving the development of analogues of the natural product 1-phenanthryl-tetrahydroisoquinoline ((-)-β-hydrastine), nonselective indolin-2-one derivatives and highly potent and selective 6-chloro-4-aminoquinazoline derivatives. Based on these experiences, we have become increasingly aware of the importance of lead compounds selection, and compounds that serve as excellent hits can guide us in target selection and significantly reduce our time and investment.

With the goal of developing selective scaffolds for designing novel PAK4 inhibitors, a structure-based virtual screening was performed for 750,000 compounds from the SPECS, Maybridge, Sigma-Aldrich and NCI databases by utilizing a series of protocols. Among the selected 52 compounds, four showed the moderate binding affinity when tested with a Kinase-Glo Luminescent Kinase Assay kit at 10 μM. To obtain compounds that were selective hits, we conducted a selectivity study of the four compounds within the PAK family by utilizing in silico strategies. Fortunately, SPU-106 was discovered to be a more selective inhibitor of PAK4 than PAK1, and our hypothesis was verified by subsequent experiments. The binding mode of SPU-106 to PAK1/4 and the selectivity mechanism study for the PAK4 protein are described. Moreover, the effects of SPU-106 on the proliferation and invasion of human gastric cancer cells were explored, as well as the possible underlying mechanism. Furthermore, SPU-106 was labeled with a biotin-avidin system to confirm that the compound bound to the C-terminal kinase domain of PAK4.

2. Result and discussion

2.1. Virtual screening

Virtual screening is one of the fastest and most effective methods used to find new chemotypes for diverse targets. For the purposes of time and efficiency, a virtual screening was carried out based on structural similarity and the pharmacophore. Approximately 750,000 molecules from the commercially available databases SPECS, Sigma-Aldrich, NCI and Maybridge, all of which were downloaded from the ZINC website (http://zinc.docking.org/), were selected for virtual screening (Fig. 1).

The three-dimensional pharmacophore model and the nine compounds active against PAK4 utilized in screening were generated from a previous study we conducted [17]. The nine PAK4-active compounds were used as the training set, and preliminary screening and sorting were carried out according to structural similarity rules by HiTS; the first 5% of the molecules were retained. Next, the rigid docking software FRED with the pharmacophore as a limiting condition was used to screen compounds that produced multiple conformations by Omega. Based on the cascaded screening, 52 molecules were identified and purchased for further evaluation by bioassays.

2.2. In vitro evaluation of virtual screening hits

We performed in vitro assays with the goal of investigating the effectiveness of compounds selected in our virtual screening against

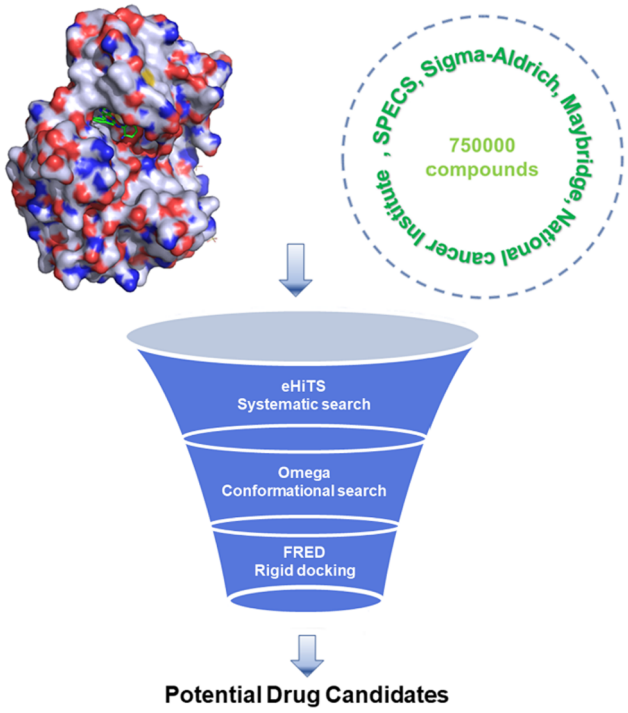

Fig. 1. Flowchart of the virtual screening procedure.

PAK4. The potency of the selected compounds against PAK4 was determined by a Kinase-Glo Luminescent Kinase Assay kit at a concentration of 10 μM (Fig. 2A). Encouragingly, 4 of the test compounds, 14# SPU-106 (Fig. 2B), 16# AK963 (Fig. S1A), 52# LC-0082 (Fig. S1D) and 23# LCH-7749944 (Fig. S1G), exhibited moderate inhibitory activity. We identified four new potential structural skeletons with PAK4 inhibitory activity through the method of virtual screening.

2.3. Protein contact atlas analysis

The representative cocrystallized structures of PAK1/4 were studied before docking simulations to determine the key amino acids and the main properties of the compounds. The asteroid plot [22] is an innovative method used to analyze interactions that utilizes the multilevel visualization of noncovalent contacts. 5XVG (PDB ID) is the cocrystal structure we obtained previously based on PAK4 and CZh-226 [19], and the asteroid plots for this structure were obtained from Protein Contact Atlas (Fig. 3A). As the residues that made direct contact (first-shell residues), Glu396, Phe397, Leu398, Asp444, Leu447 and Asp458 made large contributions to the affinity towards PAK4. Similarly, in the asteroid plots for the PAK1 protein (PDB ID: 4ZY6) [23], the cocrystalized ligand 4T6 also forms strong interactions with residues of Glu345, Tyr346, Leu347, Asp393 and Leu396 (Fig. 3B). These results provided vital information that was used by us to evaluate the interaction modes of the screened compounds.

2.4. In silico-based selectivity mechanism

Many efforts have been made in the research of PAK4 kinase inhibitors by our group. Based on our understanding and the high degree of sequence homology between PAK1 and PAK4, we hoped to achieve selectivity in the interaction between PAK1 and PAK4 through subsequent structural modification. To accelerate the progress of the project, we are now more inclined to obtain a compound with a certain selectivity and design specific PAK4 inhibitors based on the selective hit compound. Therefore, the study of the four active compounds was carried out with computational strategies that combine molecular

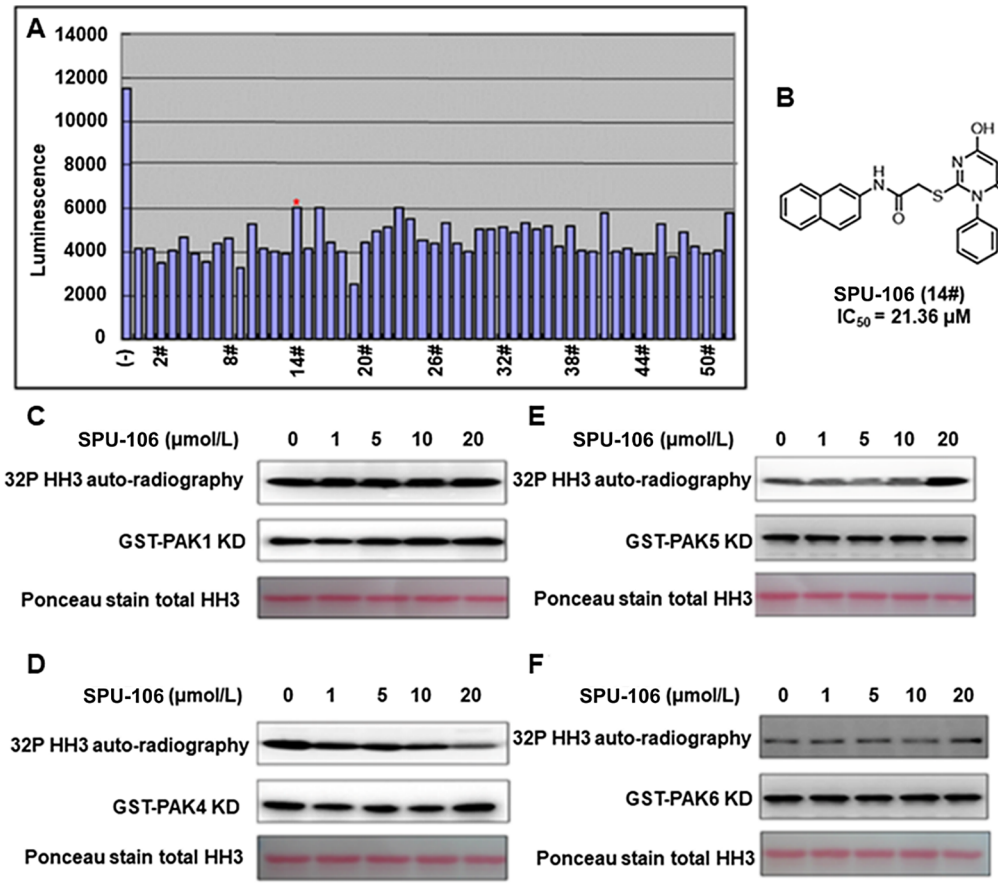

Fig. 2. SPU-106 is a selectivity PAK4 inhibitor. (A) The preliminary bioassay screening of the 52 compounds selected from the virtual screening by Kinase-Glo Luminescent Kinase Assay. (B) Chemical structure of SPU-106. (C) SPU-106 has no inhibitory effect on PAK1 kinase activity. (D) SPU-106 significant inhibits PAK4 kinase activity in vitro. (E) SPU-106 has no inhibitory activity on PAK5. (F) SPU-106 has no inhibitory activity on PAK6. The indicated concentrations of SPU-106 were pre-incubated with the four PAK family, afterward the kinase assays were performed.

docking and molecular dynamics simulations to predict the selectivity for PAK1/4.

Based on the docking results, the binding modes of AK963 and LCH-7749944 with PAK1 are consistent with those with PAK4 (Fig. S1A-F), and both ligands form key interactions with the conserved residues Leu398 (PAK4) and Leu347 (PAK1) in the hinge region. In addition, the docking scores of the two kinases did not appear to be different (Table S1). In fact, AK963 was found to exhibit inhibitory activity towards PAK1 in subsequent studies [24]. The PAK1 inhibitory activity of LCH-7749944 was verified in a subsequent study, and an optimized selective PAK4 inhibitor, CZH-226, was obtained by subsequent structural modification [3,19].

The active pockets in PAK family members are very large, which results in flexible compounds with more freedom in terms of their conformations. The compounds LC-0082 and **SPU-106** bind to PAK1/4 via two entirely different conformations. The interactions of the two

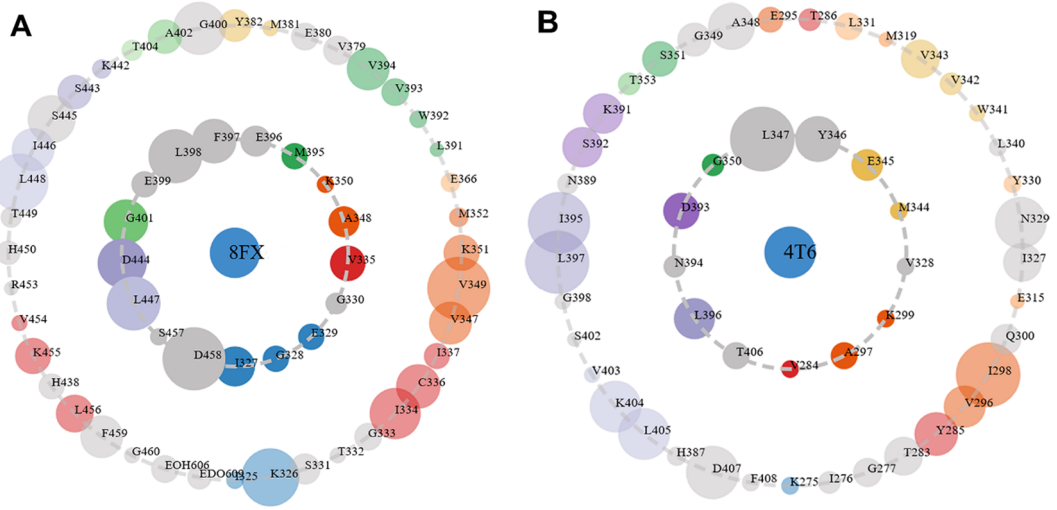

Fig. 3. Visualization and analysis of protein–ligand contacts. (A) The asteroid plots of PAK4 cocrystal structure (PDB ID: 5XVG). (B) The asteroid plots of PAK1 cocrystal structure (PDB ID: 4ZY6). Asteroid plot with the ligand highlighted in blue (central node). Directly contacting residues (first-shell residues) are shown in the inner circle, and the residues that contact these but not the ligand (second-shell residues) are shown in the outer circle. The residues are colored according to their secondary structures, and the size of each circle is scaled to denote the number of atomic contacts.

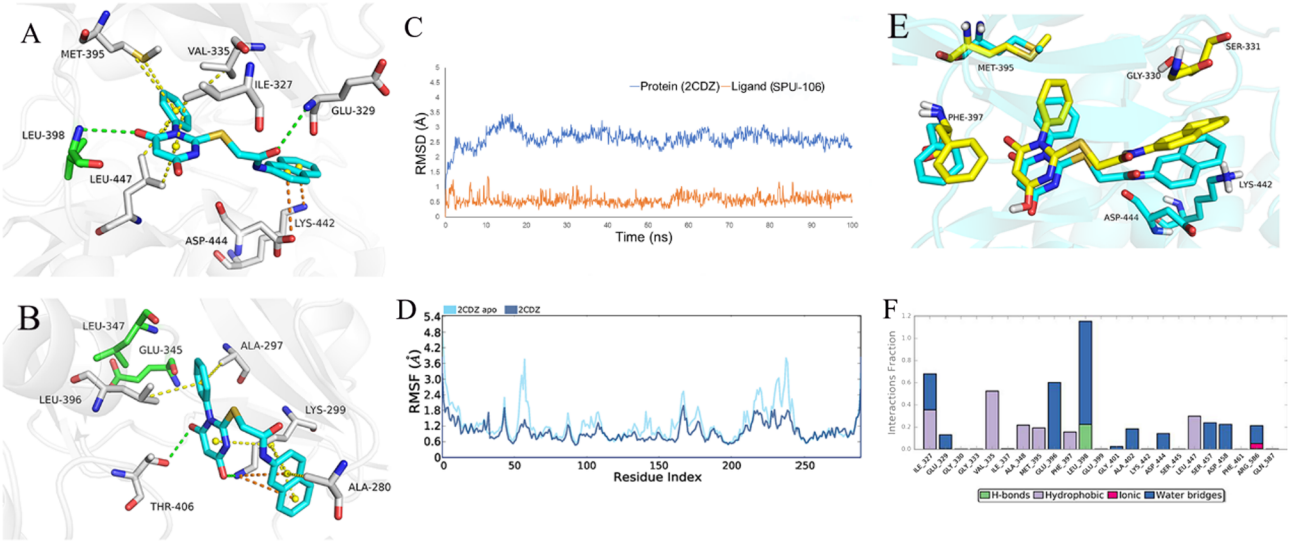

Fig. 4. Computer simulations analysis of SPU-106. (A) Predicted binding mode of compound SPU-106 with PAK4 (PDB ID: 2CDZ). (B) Predicted binding mode of compound SPU-106 with PAK1 (PDB ID: 4ZY6). (C) RMSD of PAK4 protein backbone atoms (blue line) and SPU-106 (orange line) monitored throughout the 100 ns molecular dynamics simulations. (D) Comparison of RMSF of each residue of 2CDZ apo (cyan line) and complex (blue line) throughout the 100 ns MD simulation. (E) Comparison of the docking predicted (cyan) and MD predicted (yellow) poses for the complex. (F) Normalized stacked bar chart representation of interactions and contacts over the course of the MD trajectories for complex.

compounds with PAK4 were more in line with our expectations and were very different from the traditional binding mode of PAK1. The carbonyl group of SPU-106 and the hydroxyl and carbonyl groups of LC-0082 formed typical hydrogen bond interactions with the conserved residue Leu398 in the PAK4 hinge region (Fig. 4A: PAK4/SPU-106; Fig. S1H: PAK4/LC-0082), which is very important for the affinity of compounds towards PAK4. However, the two ligands did not form any key interactions with PAK1 (Fig. 4B: PAK1/SPU-106; Fig. S1I: PAK1/LC-0082). Moreover, the docking scores of the compounds with PAK4 are significantly better than those with PAK1 (Table S1). Thus, we speculate that LC-0082 and SPU-106 are selective PAK4 inhibitors. Although we determined that LC-0082 showed a certain selectivity, no further modification experiments were performed except for basic pharmacological experiments [25] due to the increased influence of molecular weight and chiral factors. To further understand the binding mode and stability of the PAK4-SPU-106 complex, the subsequent focus of research was molecular dynamics simulation.

2.5. Molecular dynamics simulation of the PAK4-SPU-106 complex

Molecular dynamics (MD) simulation was carried out to confirm the stability of the complex in a near physiological environment. The 100 ns MD simulations of PAK4/SPU-106 were implemented to explore the stability of the possible binding modes predicted by the previous docking analysis of the reference structure. The trajectory data of the MD simulation were subjected to analysis according to three factors: Root Mean Square Deviation (RMSD), Root Mean Square Fluctuation (RMSF) and potential energy. The RMSD of the PAK4-SPU-106 complex underwent more fluctuations between 0 and 30 ns and varied between 1.0 and 3.4 Å, and it tended to be stable at approximately 2.5–3.0 Å during the last 70 ns (Fig. 4C), which indicates that the complex was relatively stable for the duration of the MD trajectory. The RMSF of the complex was found to have the lowest average RMSF value, while the fluctuation of apo PAK4 (PDB: 2CDZ) produced the higher RMSF value (Fig. 4D), suggesting that compound SPU-106 plays an important role in stabilizing the PAK4 protein. The interaction of the PAK4/SPU-106 complex was monitored throughout the simulation, and we could see that water bridge contacts comprised most of the protein-ligand interactions according to the MD simulation results (Fig. 4F). A water molecule replaced Leu398 to form a hydrogen bond with the carbonyl oxygen atom in the pyrimidone ring of the ligand, accounting for 80.3% of the entire MD simulation, and the direct hydrogen bond formed between pyrimidinone and Leu398 accounted for only 19.7%. The residues Ile327, Glu329, Glu396, Ala402, Asp444, Ser457, Asp458 and Arg586 were observed to participate in water bridge interactions. Several hydrophobic amino acids in PAK4, including Ile327, Val337, Ala348, Met395, Phe397 and Leu447, formed strong hydrophobic interactions with the compound. Regardless of the selective contribution of these amino acid residues, they played a vital role in stabilizing protein-ligand binding.

The final binding mode obtained from the 100 ns MD simulations is shown in Fig. 4E. In the three-dimensional action diagram, the dynamic and docking conformations changed substantially for both the ligand and the protein. In the hinge region of the protein, Phe397 shows a deflection towards pyrimidone that is induced by the ligand, and a π-π stacking interaction is formed with pyrimidone; these interactions were nonexistent in the docking results. The N-(naphthalen-2-yl)acetamino group in the tail of SPU-106 was also deflected considerably and oriented towards Gly330 and Ser331 to form hydrophobic contacts, which inhibited the formation of the π-ion interactions with Asp444 and Lys442 observed in the docking study. The results of the analysis of the MD simulation are more in line with our expectations of the binding mode because the system used was more representative of the real physiological environment. The studies of docking and MD simulation provided guidance for the further development of the ligand. The phenyl on the pyrimidone was a modified group that was replaced by smaller hydrophobic groups and may be a better choice for modification. According to the properties of the ATP binding pocket, N-(naphthalene-2-acyl) acetamide can be substituted by hydrophilic groups with hydrogen donor or receptor elements that could interact with Asp444, Asp458 or Lys442 to improve the inhibitory activity.

2.6. Selectivity evaluation of the PAK families

To better evaluate the in vitro activity and selectivity of the promising candidate compound SPU-106, kinase assays were performed. The compound SPU-106 showed moderately potent inhibitory activity against PAK4 (IC_{50} = 21.36 μM). We further detected the inhibitory effects of SPU-106 on PAK4 by immunoprecipitation and kinase assays, and the results indicated that SPU-106 effectively inhibited the

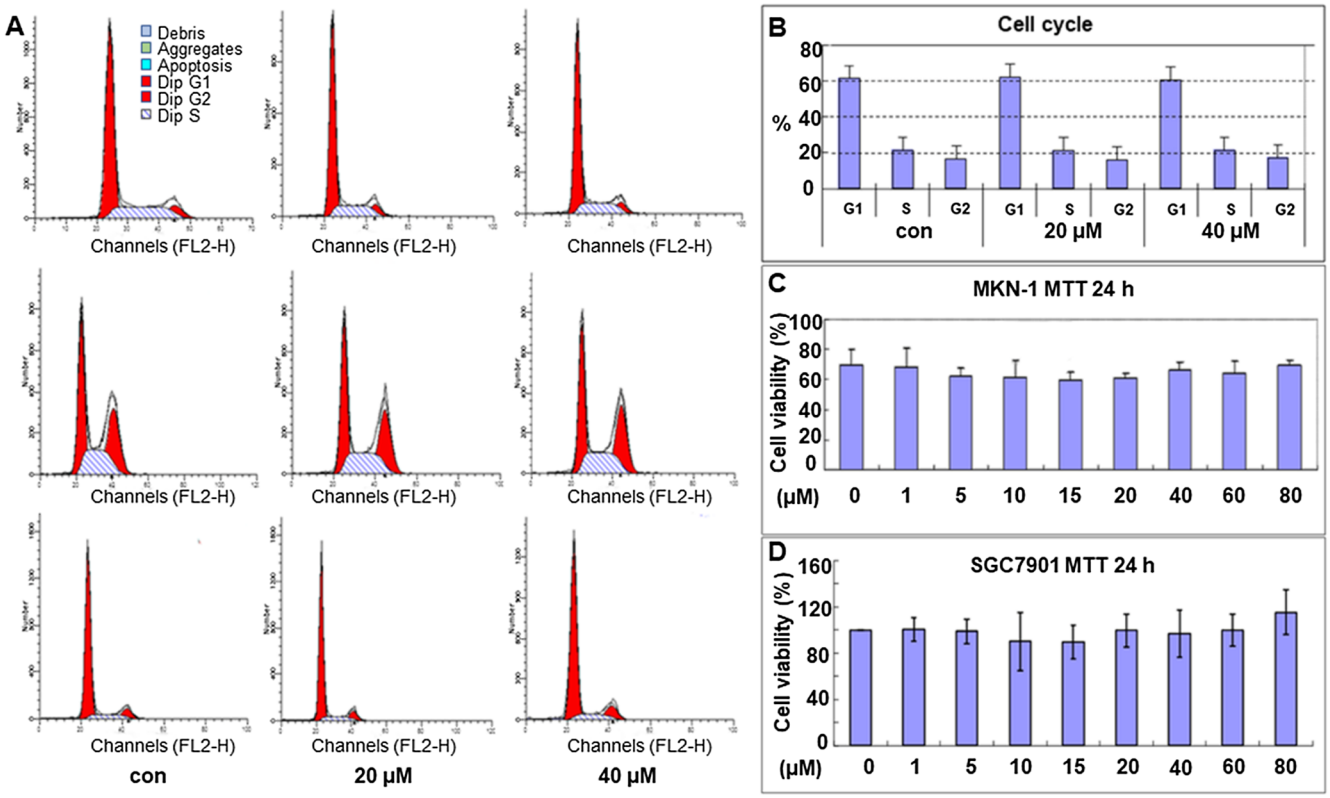

Fig. 5. SPU-106 don't suppresses proliferation in human gastric cancer cells. (A) The effect of compound SPU-106 on cell cycle in SGC7901 cells. (B). Quantitative analysis of cell cycle. (C) MTT assay showed the antiproliferative effect of SPU-106 on MKN-1 cell line. (D) MTT assay showed the antiproliferative effect of SPU-106 on SGC7901 cell line.

phosphorylation of the histone H3 substrate in a dose-dependent manner (Fig. 2D). The kinase assay results showed that the inhibitory effects of SPU-106 on other PAK family members reduced compared to its effects on PAK4, indicating that SPU-106 selectively inhibits different PAK family members, and the western blot analysis further proved the previous speculation that was based on the docking study (Fig. 2C, E, F). The success of this verification indicated that the selectivity of the compound towards PAK1/4 could possibly be predicted with computational strategies.

2.7. The cytotoxicity and cell cycle dynamics of SPU-106 in SCG7901 cells

The effect of SPU-106 on the proliferation of the gastric cancer cell lines SGC7901 and MKN-1 was examined. The experimental results were quantified with columns and show that SPU-106 has no effect on the proliferation of PAK4-overexpressing cells (Fig. 5C, D), which indicates that SPU-106 has no cytotoxic effects. To further understand the effects of SPU-106 on cells, we explored the effects of the compound on cell cycle dynamics by flow cytometry (Fig. 5A). There was no significant change in the cell cycle distribution at the maximum concentration of 40 μM.

As we mentioned in the introduction, the activation of PAK4 protects cells from apoptosis and promotes cell proliferation and metastasis. The upregulation of PAK4 expression and its overexpression promote the development of tumors. This seems to be contradictory to our experimental results. We determined that there are two possible reasons for this phenomenon. One reason is that the most important physiological function of PAK4 is to influence the dynamic changes in the cytoskeleton by regulating actin assembly, which is closely related to the metastasis of cancer [26,27]. The other reason is that PAK4 not only has an important function as a protein kinase but also has functions that are independent of its kinase catalytic activity [28]. PAK4 can promote cell survival by both kinase-dependent and kinase-independent mechanisms [27,29,30]. These reasons and results suggest that the inhibition of PAK4 kinase activity may be more sensitive to tumor metastasis, but not sufficient to inhibit the tumor proliferation at experimental concentrations due to the weak activity.

2.8. SPU-106 inhibits the invasive potential of SGC7901 cells

Metastasis is the main cause of death in patients with gastric cancer. The most important function of PAK4 is to influence the assembly of the cytoskeleton. Therefore, we further explored the effect of SPU-106 on the invasion of the human gastric cancer cell line SGC7901. Fig. 6A shows an obvious decrease in the number of cells after treatment with SPU-106 for 72 h. When treatment with 20 μM SPU-106, the invasion rate was less than half of that observed in the control group. After increasing the SPU-106 concentration to 40 μM, the invasion rate was further reduced compared to that in cells treated with 20 μM SPU-106, which suggested that the inhibition of the invasion of SGC7901 cells by SPU-106 occurred in a dose-dependent manner.

2.9. Effects of SPU-106 on inhibiting the phosphorylation of PAK4 and its downstream signaling pathways

As a downstream effector of LIMK, cofilin is a key regulator of actin reorganization. PAK4 inhibits the depolymerization of actin by acting on p-LIMK and phosphorylating cofilin [31]. Hence, western blot assays were performed to detect the effect of SPU-106 on the c-Met-PAK4-LIMKl-cofilin signaling pathway. As shown in Fig. 6C, when SGC7901 cells were exposed to SPU-106 (20, 40, 60, or 80 μM) for 24 h, SPU-106 significantly attenuated p-PAK4 levels in a dose-dependent manner, and the phosphorylation of LIMK1 and cofilin was partially and dose-dependently inhibited. In previous research, we discovered that PAK4-mediated SCG10 phosphorylation is closely related to the metastasis of gastric cancer [32]. Therefore, we performed immunoprecipitation

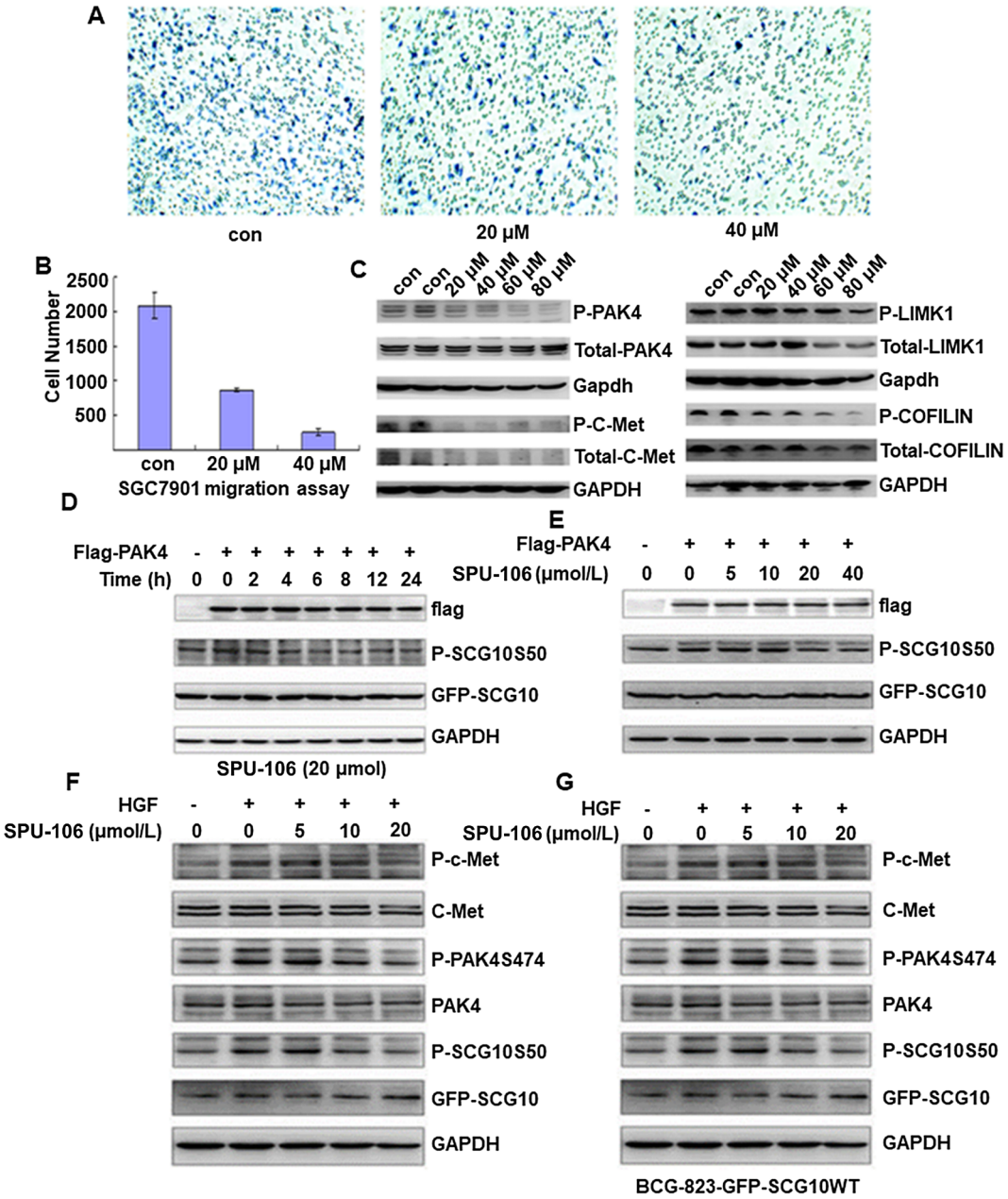

Fig. 6. SPU-106 suppresses invasion of human gastric cancer cells. (A) Transwell assay was performed to show the effect of indicated concentrations of SPU-106 on SGC-7901 gastric cancer cell invasion. (B) Quantitative analysis of invasion. (C) Compound SPU-106 inhibits phosphorylation level of PAK4 and the phosphorylation of downstream effector proteins LIMK1 and cofilin in SCG7901 cell line. (D) SGC-7901 cells stably overexpressing GFP-SCG10 were transiently transfected with Flag-PAK4. Western blot analysis was carried out for the indicated amount of time. (E) SGC-7901 cells stably overexpressing GFP-SCG10 were transiently transfected with Flag-PAK4. Western blot analysis was carried out after treatment with different concentrations of SPU-106. (F) Western blot assay of the c-Met/PAK4/SCG10 signaling pathway treated with different concentrations of compound in SGC7901 cell line. (G) Western blot assay of the c-Met/PAK4/SCG10 signaling pathway in BCG823 cell line.

assays to test the effect of SPU-106 on the phosphorylation of SCG10. Fig. 6D shows that SPU-106 significantly inhibited the phosphorylation of SCG10 in a time-dependent manner in SGC7901 cells transiently transfected with Flag-PAK4. When cells transiently transfected with Flag-PAK4 were treated with different concentrations of the compound, the phosphorylation level of SCG10 was inhibited in a dose-dependent manner (Fig. 6E). A western blot assay of the c-Met/PAK4/SCG10 signaling pathway was also performed with different concentrations of SPU-106 in the SGC7901 and BCG823 cell lines (Fig. 6F, G). We observed from the two western blot analyses that SPU-106 had no effect on the upstream protein c-Met. However, it could effectively inhibit the phosphorylation levels of PAK4 and the downstream protein SCG10, which have significant effects on the inhibition of the invasion of SGC7901 gastric cancer cells.

2.10. Biotin-avidin system assays

The biotin-avidin system is used to indirectly study the interaction between two biomolecules. Biotin interacts with targeted molecules without interfering with the interactions between the target molecule and other molecules; avidin is used to recognize and determine the localization of target molecules. Today, the biotin-avidin system is applied in research and diagnostics as well as medical devices and pharmaceuticals. Biomarker technology has been widely used in drug

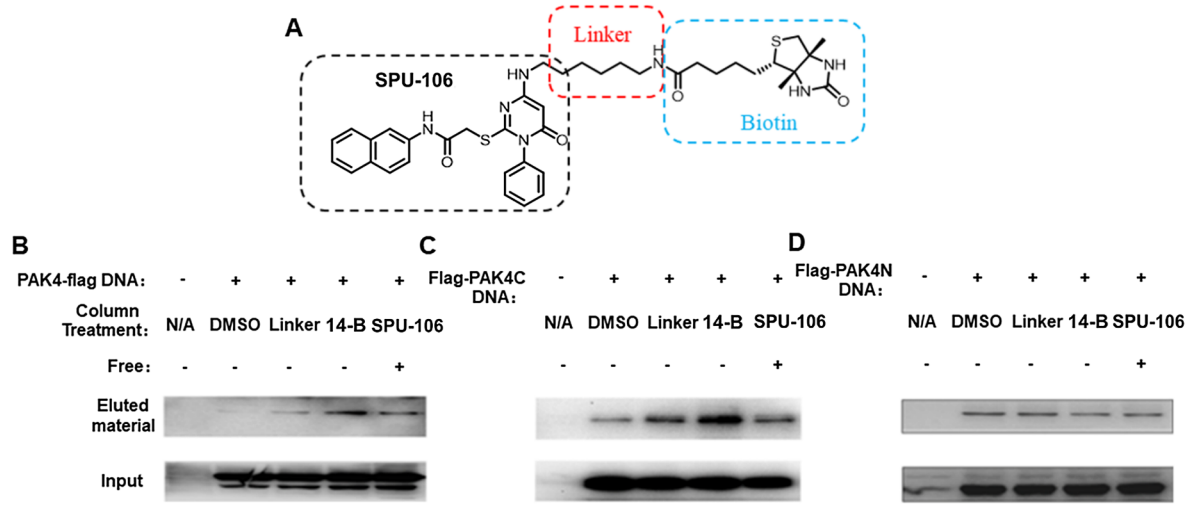

Fig. 7. Molecular probe revealed the binding with C-terminal of PAK4. (A) Design of biotin labeled compound. SPU-106 and biotin were connected by hexane-1,6-diamine as linker. (B) The western blot analysis of the full-length Flag-PAK4 DNA transfected HEK293 cells with different compounds. (C) The western blot analysis of the Flag-PAK4C with different compounds. (D) The western blot analysis of the Flag-PAK4N with different compounds.

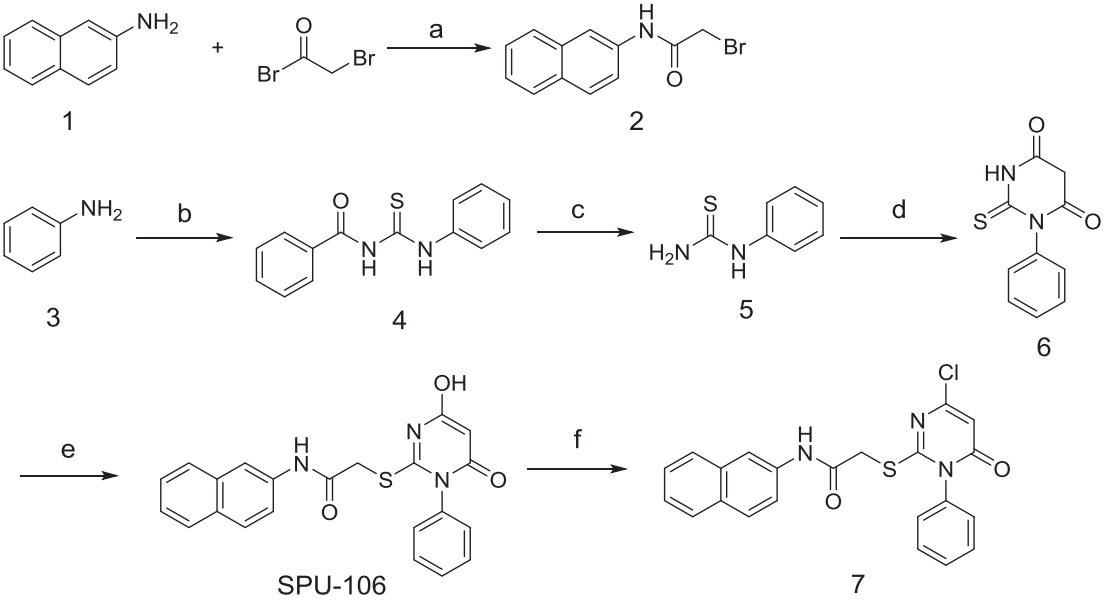

Scheme 1. General procedures used to synthesize compound SPU-106.

research. The labeled small molecules or proteins possessing biological activities with biotin can be used to determine the molecular targets of drugs, purify labeled proteins and study the mechanisms of drug action [33,34].

To further confirm the mechanism of action involved in the binding of SPU-106 to PAK4 kinase, we designed a biomarker molecule as a molecular probe. By analyzing the structural characteristics and the binding mode of SPU-106, it was found that the hydroxyl group in the pyrimidinone ring is in a position where chemical derivatization is relatively easy and does not have a significant impact on the affinity between SPU-106 and PAK4 according to the docking conformation. Therefore, we designed a biotin-labeled compound, 14-B, that links biotin and the pyrimidinone hydroxyl group via hexane-1,6-diamine to further explore the binding model of the ligand and protein (Fig. 7A).

To determine the binding of SPU-106 to the PAK4 protein, 14-B was incubated with a cell lysate by a specific method after lysing HEK293 cells transfected with the full-length flag-PAK4 DNA. In the western blot analysis (Fig. 7B), it was observed that the chemiluminescence in the fourth group was more intense than that in the first three control groups, indicating that 14-B could effectively bind to the full-length PAK4 protein and be captured by avidin. Moreover, the chemiluminescence was significantly reduced when SPU-106 and 14-B were added at the same time, which indicated that SPU-106 competitively prevented the binding of 14-B. All of the above analyses indicate that the SPU-106 compound can interact with the full-length PAK4 protein.

Then, we tested the interaction of SPU-106 with the C-terminus of PAK4 (Flag-PAK4C) and N-terminus of PAK4 (Flag-PAK4N) proteins. The detection results for Flag-PAK4C were similar to those of the full-length protein (Fig. 7C); the binding of the captured protein was maximized when 14-B was added, and the addition of SPU-106 competitively prevented the binding of 14-B. However, the chemiluminescence was not enhanced when 14-B was added compared to that observed in the top three groups, while the results in the competitive experimental group did not significantly change for N-terminal detection (Fig. 7D). These results indicate that the compound interacted with the C-terminus and had no significant effect on the N-terminus of PAK4. Through these experimental analyses, we can conclude that our compound could effectively bind to the C-terminal kinase domain of PAK4

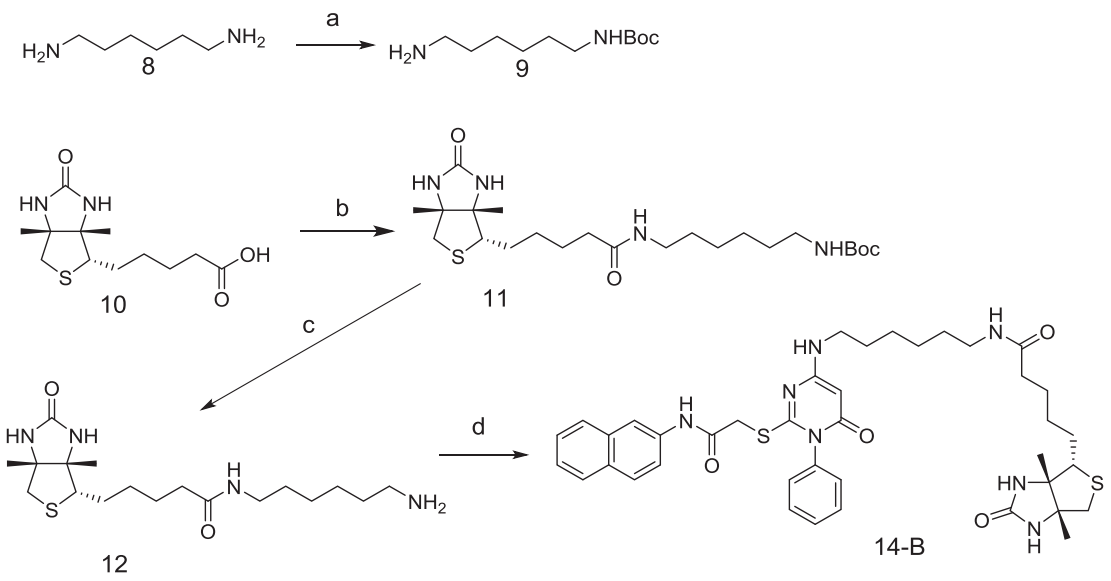

Scheme 2. General procedures used to synthesize compound 14-B.

and inhibit its phosphorylation activity.

2.11. Chemistry

The synthesis of **SPU-106** and **14-B** were carried out according to the procedures shown in Scheme 1 and Scheme 2. Commercially obtained 2-naphthylamine was reacted with 2-bromoacetyl bromide to yield intermediate **2**. Treatment with aniline, benzoyl chloride and ammonium thiocyanate produced the corresponding N-(phenylcarbamothioyl) benzamide **4**, which was subsequently hydrolyzed under basic conditions to yield the 1-phenylthiourea **5**. In an ethanol solution with sodium ethoxide, **5** and diethyl malonate underwent a cyclization reaction to obtain a key intermediate, 1-phenyl-2-thioxodihydropyrimidine-4,6(1H,5H)-dione. The key intermediate **6** was reacted with **2** under basic conditions to yield the compound **SPU-106**.

The compound **SPU-106** was treated with phosphorus oxychloride to obtain the chlorinated derivative **7**. Intermediate **9** was obtained by using 1,6-hexanediamine and a single *t*-butyloxycarboryl (Boc) group to protect product **10**. Upon amidation with biotin in the presence of 1-Ethyl-3-(3-dimethylaminopropyl)carbodiimide hydrochloride (EDCI) and 1-Hydroxybenzotriazole (HOBt), intermediate **10** was converted to intermediate **11**. The deprotection of **11** under standard conditions yielded the desired product **12** at a good yield. The subsequent condensation of **12** with the pyrimidone **7** in the presence of triethylamine produced the compound **14-B**.

Reagents and conditions: (a) Pyridine, r.t, 4 h (72%); (b) NH_4SCN, benzoyl chloride, acetone, reflux, 1 h; (C) 10% aq. NaOH in water, 80 °C, 0.5 h (83.1%); (d) sodium ethoxide, diethyl malonate, ethanol, reflux, 10 h (70.9%); (e) **2**, sodium hydroxide, ethanol, 40 °C, 5 h (62.5%); (f) $POCl_3$, reflux, 2 h (38.5%)

Reagents and conditions: (a) di-tert-butyl decarbonate, dichloromethane, r.t, 16 h (47.3%); (b) **9**, DCC, HOBT, DMF, r.t, 10 h (73.5%); (c) 4 M HCl solution in dioxane, ethyl acetate, r.t, 2 h (93.7%); (d) **7**, Et_3N, 80 °C, 5 h (14.5%).

3. Conclusion

In this study, virtual screening was carried out to identify new scaffolds for PAK4 inhibitors. Four out of fifty-two purchased compounds showed moderate inhibitory potency against PAK4 in actual biochemical assays. To obtain selective hit compounds, a molecular docking strategy was utilized for contraposing the four molecules, and the compound SPU-106 was identified for further development into a selective PAK4 inhibitor. Subsequently, molecular dynamics simulations confirmed the reliability of the docking conformations and provided theoretical support for future modifications. Following the in silico experiments, we performed a series of western blotting analyses to further confirm the selectivity of the compound SPU-106 towards PAK family members. The cell-based tests show an absence of anti-proliferative activity and effective anti-invasive activity in SGC7901 gastric cancer cells. The mechanism and effectiveness were validated through two anti-invasion signaling pathways, PAK4/LIMK1/COFILIN and PAK4/SCG10; the latter was a signaling pathway discovered during our previous research. The binding of PAK4C and SPU-106 was further confirmed by utilizing a biotin-avidin system. In conclusion, the use of a biosynthetic approach combined with an in silico methodology allowed fast and cost-efficient lead identification in the drug discovery process. Therefore, we have demonstrated that compound SPU-106 is a potent and selective candidate PAK4 inhibitor. The innovative structure skeleton of SPU-106 provides a new chemotype for the development of selective PAK4 inhibitors and our study provided a hit compound that could be developed into a new effective therapeutic agent for the treatment of the metastasis of advanced tumors.

4. Experimental procedures

4.1. General methods for chemistry

All reagents or solvents were purchased from commercial suppliers without further purification. All reactions were detected by thin layer chromatography (TLC) and completely terminated based on the consumption of one starting material with fluorescence F-254 and visualized with UV light, Dragendorff reagent or iodine stain. Column chromatography was performed using silica gel (200–300 mesh). The NMR spectra were recorded on Bruker ARX-400 NMR spectrometer and referenced to tetramethylsilane. Waters Quattro micro API triple quadrupole tandem mass spectrometer was used for mass spectrometry, equipped with electrospray ion source (ESI source) and Masslynx 4.1 data acquisition software.

4.1.1. 2-bromo-N-(naphthalen-2-yl) acetamide **(2)**

To a solution of naphthalen-2-amine (5 g, 53.7 mmol) in acetonitrile (100 mL) was added pyridine (6.4 g, 80.5 mmol) as an acid-binding agent, while maintaining the temperature below 5 °C, followed by addition of bromoacetyl bromide (13 g, 64.4 mmol) via dropwise addition. After addition, the mixture was stirred for 1 h at this temperature,

and 2.5 h at room temperature. Pour the reaction solution into 300 mL of ice water with stirring to cause solid precipitation. Filter the suspension, wash it with water and dry in vacuum oven at 50 °C to afford crude product 2 (8.3 g, 72.2%) as white solid, which was used in the next step without further purification. ESI-MS: *m/z* $[M-H]^-$: 262.9.

*4.1.2. 1-phenylthiourea **(5)***

To a solution of ammonium thiocyanate (11.4 g, 0.15 mol) in acetone (80 mL) was added benzoyl chloride (16 mL, 0.14 mol) within 10 min in three-necked flask. After the addition was completed, the mixture was heated to reflux for 15 min. Heating was stopped and the aniline (9.3 g, 0.1 mol) in acetone (30 mL) was added as rapidly as possible maintaining a vigorous reflux. After addition, the mixture was healed to reflux for 30 min, then poured into excess ice water with vigorous stirring. The solid was collected and washed with liberal water, followed by cold H2O/MeOH (1/1). The product was used to hydrolysis to the thioureas without further purification.

The appropriate *N*-(phenylcarbamothioyl) benzamide **5** was added batch in preheated (~80 °C) stirring solution of 100 mL 10% aq. NaOH. After heating for 30 min at 80 °C, the mixture was poured onto excess ice containing excess aq. HCl. The aqueous layer was alkalified with sodium carbonate to pH 8–8.5 and the white solid formed. Collect the solid by suction filtration and the residue was recrystallized from ethanol (95%) to yield white crystals (13.8 g, 83.1%) for to steps.

*4.1.3. 1-Phenyl-2-thioxodihydropyrimidine-4,6(1H,5H)-dione **(6)***

To a solution of sodium ethoxide in ethanol (4.6 g sodium was added in 200 mL ethanol) was added 1-phenylthiourea (15.2 g, 0.1 mol) and stirred until the solids dissolved. After adding diethyl malonate, the reflux was heated for 10 h. After evaporation of solvents in vacuo, the residue was dissolved in water (50 mL) and filter to remove solid residue. The filtrate was acidified with 6 N hydrochloric to pH 4–5 and yellow precipitation formed. Collect the solid by suction filtration and the residue was recrystallized from ethanol to give yellow crystals (15.6 g, 70.9%). ESI-MS: *m/z* $[M+H]^+$: 219.3.

*4.1.4. 2-((4-Hydroxy-6-oxo-1-phenyl-1,6-dihydropyrimidin-2-yl)thio)-N-(naphthalen-2-yl)acetamide **(SPU-106)***

To a solution of 1-phenyl-2-thioxodihydropyrimidine-4,6(1H,5H)-dione (0.5 g, 2.27 mmol) in absolute ethyl alcohol (20 mL) was added sodium hydroxide (0.11 g, 2.7 mmol). After stirring for 10 min, 2-bromo-N-(naphthalen-2-yl) acetamide (0.49 g, 2.27 mmol) was added batch and the mixture was stirred at 40 °C for 5 h. Pour the reaction solution into 40 mL of ice water and acidified with 0.5 N hydrochloric to pH 6. The mixture was filtered, and purified by silica gel chromatography (MeOH:DCM = 1:20) to provide **SPU-106** (0.5 g, 62.5% yield) as a white solid. ESI-MS: *m/z* $[M+H]^+$: 404.19, $[M-H]^-$: 402.17. 1H NMR (400 MHz, DMSO-d_6) δ 11.55 (s, 1H), 10.37 (s, 1H), 8.25 (d, J = 2.0 Hz, 1H), 7.88–7.78 (m, 3H), 7.55 (ddd, J = 5.5, 4.1, 1.6 Hz, 4H), 7.47 (ddd, J = 8.2, 6.8, 1.3 Hz, 1H), 7.40 (ddd, J = 8.2, 6.8, 1.4 Hz, 1H), 7.38–7.35 (m, 2H), 5.32 (s, 1H), 4.08 (s, 2H).

*4.1.5. 2-((4-Chloro-6-oxo-1-phenyl-1,6-dihydropyrimidin-2-yl)thio)-N-(naphthalen-2-yl) acetamide **(7)***

SPU-106 (0.5 g) was added to phosphorus oxychloride (10 mL) and the mixture was refluxed for 2 h. The reaction mixture was evaporated in vacuo and the residue was dissolved in 5% sodium bicarbonate solution (20 mL). The mixture was extracted with ethyl acetate (20 mL × 3), the combined organic was washed with water, brine, dried over anhydrous sodium sulfate and concentrated under reduced pressure. The residue was purified silica gel chromatography (PE:EA = 2:1) to provide yellow solid (0.2 g, 38.5%). ESI-MS: *m/z* $[M+H]^+$: 422.2.

*4.1.6. Tert-butyl (6-aminohexyl) carbamate **(9)***

Hexane-1,6-diamine **8** (11.17 g, 127 mmol) was added in dichloromethane (170 mL). The solution of di-tert-butyl decarbonate (2.77 g, 12.7 mmol) in dichloromethane (50 mL) was dropped slowly over 1 h below 0 °C. After the addition was complete, the mixture was stirred another 16 h at room temperature. The reaction solution was washed by water (100 mL × 2), brine (100 mL × 2), dried over anhydrous sodium sulfate. After concentrated under reduced pressure. The residue was purified silica gel chromatography (DCM:MeOH = 20:1) to provide wax yellow solid (1.3 g, 47.3%). ESI-MS: *m/z* $[M+H]^+$: 217.3.

*4.1.7. Tert-butyl (6-(5-((3aS,4S,6aR)-3a,6a-dimethyl-2-oxohexahydro-1H-thieno[3,4-d] imidazol-4-yl) pentanamido)hexyl)carbamate **(11)***

A solution of biotin (0.56 g, 2.3 mmol), DCC (0.57 g, 2.76 mmol) and HOBt (0.06 g, 0.46 mmol) in DMF (20 mL) was stirred at 0 °C for 2 h. Then tert-butyl (6-aminohexyl) carbamate **9** (0.6 g, 2.8 mmol) was added and the mixture was stirred for another 10 h at room temperature. The reaction mixture was filtered, and the filtrate was purified by flash column chromatography (DCM:MeOH = 50:1–10:1) to provide white solid (0.75 g, 73.5%). ESI-MS: *m/z* $[M+H]^+$: 443.4.

*4.1.8. N-(6-aminohexyl)-5-((3aS,4S,6aR)-3a,6a-dimethyl-2-oxohexahydro-1H-thieno[3,4-d] imidazol-4-yl) pentanamide **(12)***

To a stirred slurry of intermediate **11** (15.0 g, 35.0 mmol) in ethyl acetate (30 mL) was dropwise added 4 M HCl solution in dioxane (3.8 mL). After addition, the mixture was stirred for 2 h at room temperature. The reaction solution was concentrated under vacuum and recrystallized from MeOH/Et2O to yield white solid (0.6 g, 93.7%). ESI-MS: *m/z* $[M+H]^+$: 343.3. 1H NMR (300 MHz, DMSO-d_6, ppm) δ: 1.23–1.64 (m, 14H), 2.04 (t, J = 7.3 Hz, 2H), 2.57 (d, J = 12.4 Hz, 1H), 2.81 (dd, J = 12.4 Hz, J = 5.1 Hz, 1H), 2.87–2.89 (m, 1H), 2.99 (q, J = 6.6 Hz, 2H), 3.06–3.12 (m, 1H), 3.35 (m, 1H, overlapped with H2O), 4.10–4.14 (m, 1H), 4.28–4.32 (m, 1H), 6.37 (s, 1H), 6.42 (s, 1H), 7.79 (s, 1H).

*4.1.9. 5-((3aS,4S,6aR)-3a,6a-dimethyl-2-oxohexahydro-1H-thieno[3,4-d] imidazol-4-yl)-N-(6-((2-((2-(naphthalen-2-ylamino)-2-oxoethyl)thio)-6-oxo-1-phenyl-1,6-dihydropyrimidin-4 yl)amino)hexyl)pentanamide **(14-B)***

To a solution of **12** (0.36 g, 0.95 mmol) in anhydrous DMF (10 mL) was added 2-((4-chloro-6-oxo-1-phenyl-1,6-dihydropyrimidin-2-yl) thio)-N-(naphthalen-2-yl) acetamide (7, 0.4 g, 0.95 mmol) and Et3N (0.26 mL, 1.9 mmol). The mixture was heated to 80 °C for 5 h. After cooling to room temperature, pouring the reaction solution into 50 mL of ice water and extracted with ethyl acetate (30 mL × 3). The combined organic was washed with water (20 mL × 2), brine (30 mL × 1), dried over anhydrous sodium sulfate and concentrated under reduced pressure. The residue was purified silica gel chromatography (DCM:MeOH = 10:1) to provide white solid (0.1 g, 14.5%). ESI-MS: *m/z* $[M+H]^+$: 728.5; $[M+Na]^+$: 750.5. 1H NMR (300 MHz, CD_3OD, ppm) δ: 1.25–1.74 (m, 14H), 2.16 (t, J = 7.3 Hz, 2H), 2.68 (d, J = 12.7 Hz, 1H), 2.88 (dd, J = 12.7 Hz, J = 4.9 Hz, 1H), 2.99 (m, 2H), 3.11–3.31 (m, 3H), 3.99 (s, 2H), 4.24 (dd, J = 7.8 Hz, J = 4.4 Hz, 1H), 4.44 (dd, J = 7.7 Hz, J = 4.7 Hz), 5.16 (s, 1H), 7.35–7.49 (m, 4H), 7.54–7.59 (m, 4H), 7.75–7.84 (m, 3H), 8.20 (s, 1H).

4.2. Virtual screening

In the first round of screening, the eHiTS software was used to perform the coarse screening of the molecules in the database by applying default parameters. Nine competitive ATP inhibitors were selected to form a training set. A neural network algorithm was used to optimize the scoring function, and the initial filtering and sorting were performed according to the structural similarity rules of the compounds. Finally, the molecular structures of the top 5% of the compounds in the library were retained and used for the second round of screening.

In the next screening round, the conformations of the top 5% compounds were searched using Omega software with the following

optimization parameters: the energy window (e_window) was set to 5.0 kcal/mol, the RMSD cutoff was 0.6 Å, and 1000 output conformations were retained. Subsequently, the rigid molecular docking software FRED was utilized, and the default parameters were used. Moreover, the pharmacophore, which was constructed by LigandScout [17], was used as a limiting condition to improve the hit rate. Finally, the calculated results were evaluated by the ChemScore scoring function, and the mode of action was observed by Vida 2.

4.3. Protein and ligand preparation and molecular docking

All ligand structures were prepared by Maestro 9.0 within the Schrödinger package. The 3D structures of all the studied compounds were created with ChemBioDraw Ultra, and the initial lowest energy conformations were calculated with LigPrep. For protein preparation, the crystal structures of PAK4 (PDB code: 2CDZ) and PAK1 (PDB code: 4ZY6) were downloaded from the RCSB PDB Bank (http://www.rcsb.org/) and prepared with the Protein Preparation Wizard. The protein structure integrity was adjusted and modified and missing residues and loop segments near the active sites were built using Prime. All hydrogen atoms were added. Subsequently, the OPLS_2005 force field was used to optimize the protein energy and eliminate steric hindrance. For all dockings, the grid center was placed on the centroid of the included ligand binding site, and a 24 × 24 × 24 Å grid box size was used. All dockings were performed with Glide using the XP protocol. The docking poses were analyzed by PyMOL.

4.4. Molecular dynamics simulations

The molecular dynamics simulations of the protein-ligand complexes were performed by Desmond version 3.8 (Schrödinger suite) to explore the changes in the conformation and stability of the ligands, proteins and protein-ligand complexes through multiple trajectory diagrams. Desmond simulation involved multiple stages, including building the model systems and relaxation systems, running the simulation and analyzing the results. First, the best conformations of the protein and ligand complexes from the docking results were introduced into the Desmond (v3.8) module in the MD simulation software. After that, a simple point charge (SPC) water model was embedded in the system and the complexes were neutralized with an appropriate number of counter ions. The concentration of physiological salts remained at approximately 0.15 M, which was similar to the physiological concentration of the monovalent ions. The protein-ligand system was set as the OPLS_2005 force field [35]. After that, the system was placed in an orthogonal box with each dimension set to 10 Å. The largest interaction was set to 2000, and the convergence threshold value was set to 1 kcal/mol/Å. According to the steepest descent and the limited memory of the Broyden-Fletcher-Goldfarb-Shannon (LBFGS) algorithm, the system energy was reduced to the maximum of 5000 steps until it reached the gradient threshold of 25 kcal/mol/Å. The protein-ligand system was equilibrated at 300 K and a pressure of 1.01325 bar with the NPT ensemble. The simulation time of the relaxed system was 100 ns, and the trajectory was 4.8 ps. The root-mean-square deviation (RMSD) and energy fluctuations of the protein-ligand complex were analyzed during the MD simulation period, and the root-mean-square fluctuation (RMSF) of the side chain atoms of the PAK4 complexes were analyzed for each amino acid. The docking of the protein-ligand complexes was analyzed, and the hydrogen bonding interactions were monitored.

4.5. Kinase-Glo® luminescent kinase assay

To perform the high-throughput screening of the PAK4 inhibitors selected by virtual screening, the kinase reaction system was prepared with 4 μL histone H3, 48 ng PAK4 kinase, 1 μL cold ATP and kinase reaction buffer (50 mM HEPES, 10 mM $MgCl_2$, 10 mM $MnCl_2$, and 0.2 mM DTT), and all the target molecules were added and incubated for 45 min at 30 °C. The reactions were equilibrated for 15 min at room temperature and stopped by adding an equal volume of Kinase-Glo reagent (Promega) and incubating for 10 min at room temperature. The chemiluminescence was measured at 555 nm (20 nm emission slit) by a Cary Eclipse fluorescence spectrophotometer (Tecan) equipped with a microplate reader.

4.6. Cell lines and culture

The human gastric cancer cell lines SGC7901, MKN-1 and BCG823 were routinely cultured in DMEM (Invitrogen) with 10% fetal calf serum (Invitrogen) and penicillin/streptomycin in a humidified atmosphere with 5% CO_2 at 37 °C.

4.7. MTT assay

The anti-proliferation activities of SPU-106 were determined by MTT (3-[4,5-dimethyl-2-thiazolyl]-2,5-diphenyl-2H-tetrazolium bromide) assays. Briefly, cells (1×10^4 per well) were precultured for 24 h in 96-well plates and then treated with different concentrations of compound for 24 h. The MTT solution (0.5%) was added to each well. After another 4 h of incubation at 37 °C, the formazan that had formed was extracted by DMSO. After shaking the plates for 15 min, the absorbance at 595 nm was measured using a microplate reader (Bio-Rad).

4.8. Flow cytometry analysis

Cells were plated in six-well tissue culture plates (1×10^6 cells per well), and the degree of cell cycle arrest was analyzed by flow cytometry. After incubation with different concentrations of SPU-106 (20 and 40 μM) for 72 h, the degree of cell cycle arrest was analyzed with a FACS Vantage flow cytometer with the CellQuest acquisition and analysis software program (Becton Dickinson and Co., San Jose, CA). Gating was used to exclude cell debris, doublets and clumps.

4.9. Kinase assays

The 30 μM kinase reaction system was prepared with 4 μL histone H3 (Roche), 48 ng PAK4 kinase, and kinase reaction buffer (50 mM HEPES, 10 mM $MgCl_2$, 2 mM $MnCl_2$, 0.2 mM DTT, 2.5 μL ATP, and 0.5 μL ^{32}P-ATP) and incubated with different concentrations of SPU-106 for 1 h at 30 °C. The reaction was terminated by adding 6 μL 6x SDS Loading Buffer. The proteins were transferred onto PVDF membranes. The ^{32}P-labeled proteins were visualized by autoradiography with a Molecular Imager RX (Bio-Rad). To ensure equal amounts were loaded, PAK4 was detected by immunoblotting analysis, and histone H3 was detected by Ponceau staining. To determine the direct chemical effects on PAK family member activity in vitro, commercially obtained PAK1, PAK4, PAK5 and PAK6 kinases (Invitrogen) were preincubated with the indicated concentrations of compounds. The kinase reactions were initiated by the addition of histone H3 and a mixture of 1 mM ATP and [γ-^{32}P] ATP.

4.10. Cell invasion assay

Cell invasion assays with Matrigel were performed using modified Boyden chambers with polycarbonate nucleopore membranes (6.5 mm in diameter, 8 μm pore size, 100 μg/cm2 Matrigel). Precoated filters were rehydrated with 100 μL medium, and 1×10^5 cells were suspended in serum-free medium with different concentrations of SPU-106 and placed onto the upper part of each chamber, whereas 600 μL DMEM containing 10% serum was used as a chemoattractant in the lower chamber. After incubating for 18 h at 37 °C, the cells that had not invaded were removed from the upper side of the membrane with a cotton swab, and the invading cells on the lower surface of the

membrane were fixed, stained, photographed and counted under high-power magnification.

4.11. Western blot analysis

To determine the expression level of related proteins, SGC7901 and BCG823 cell lines were treated with SPU-106 for 4 h, and whole cell extracts were prepared from 1×10^6 cells in RIPA lysis buffer (150 mM NaCl, 50 mM Tris/HCl, pH 7.4, 0.25% Na-deoxycholate, 1 mM EDTA, 1% Nonidet P-40 and protease inhibitor cocktail). Equivalent amounts of protein were subsequently separated by SDS − PAGE and transferred to PVDF (polyvinylidene fluoride) membranes. The membranes were blocked with nonfat dry milk in TBS-T (20 mM Tris, pH 7.4, 137 mM NaCl, and 0.05% Tween-20) and incubated at 4 °C with specific primary antibodies for 3 h. The membranes were washed with TBS-T 3 times and incubated with secondary antibodies (LIMK1, phospho-LIMK1, cofilin, phospho-cofilin, PAK4, phospho-PAK4, C-met, P-C-met, SCG10, and phospho-SCG10) for 2 h at room temperature. The immunoreactive proteins were detected by chemiluminescence (ECL, Pierce Technology). To ensure equal loading, the membrane was stripped and detected with GAPDH antibody.

4.12. Biotin-avidin system assay

HEK293 cells were plated in a 10 cm culture dish at the appropriate ratio. The next day, Flag-PAK4, Flag-PAK4N and Flag-PAK4C were transfected into the cells by lipofection, and it was verified that these were expressed as proteins in cells. After incubation for 36 h, the proteins were extracted by nondenaturing reagents. Streptavidin beads were prewashed three times according to the manufacturer's instructions and incubated at room temperature for 1 h with the total proteins to isolate the proteins that specifically bound to the beads. The sample was centrifuged at 3400 rpm for 2 min at 4 °C to pellet the beads before incubation with PAK4 antibody. Then, supernatants with equal amounts of protein were incubated with different additives (including DMSO, a biotin linker, the probe (14-B), and the probe combined with SPU-106) for 1 h. Streptavidin (30 μL) was added to each protein sample and incubated with stirring at 4 °C overnight. The sample was centrifuged, and the precipitated proteins were washed 3 times with lysate buffer for 10 min each time. The precipitated proteins were denatured in 30 μL 2x SDS loading buffer, separated by SDS–PAGE and transferred to a PVDF membrane, and they were then analyzed by western blot.

4.13. Statistical analysis

SPSS 16.0 was used for all statistical analyses, and the results were considered significant when the P value was less than 0.05.

Acknowledgements

The work was financially supported by the National Natural Science Foundation of Liaoning province (Grant No. 20170540854). Virtual Lab for Medicinal Chemistry Education from Liaoning Province.

Appendix A. Supplementary material

Supplementary data to this article can be found online at https://doi.org/10.1016/j.bioorg.2019.103168.

References

[1] E. Manser, T. Leung, H. Salihuddin, Z. Zhao, L. Lim, A brain serine/threonine protein kinase activated by Cdc42 and Rac1, Nature 367 (1994) 40–46.
[2] L.E. Arias-Romero, J. Chernoff, A tale of two Paks, Biol. Cell 100 (2008) 97–108.
[3] J. Zhang, J. Wang, Q. Guo, Y. Wang, Y. Zhou, H. Peng, M. Cheng, D. Zhao, F. Li, LCH-7749944, a novel and potent p21-activated kinase 4 inhibitor, suppresses proliferation and invasion in human gastric cancer cells, Cancer Lett. 317 (2012) 24–32.
[4] M. Radu, G. Semenova, R. Kosoff, J. Chernoff, PAK signalling during the development and progression of cancer, Nat. Rev. Cancer 14 (2014) 13–25.
[5] M.G. Callow, F. Clairvoyant, S. Zhu, B. Schryver, D.B. Whyte, J.R. Bischoff, B. Jallal, T. Smeal, Requirement for PAK4 in the anchorage-independent growth of human cancer cell lines, J. Biol. Chem. 277 (2002) 550–558.
[6] Y. Liu, H. Xiao, Y. Tian, T. Nekrasova, X. Hao, H.J. Lee, N. Suh, C.S. Yang, A. Minden, The pak4 protein kinase plays a key role in cell survival and tumorigenesis in athymic mice, Mol. Cancer Res. 6 (2008) 1215–1224.
[7] P.R. Molli, D.Q. Li, B.W. Murray, S.K. Rayala, R. Kumar, PAK signaling in oncogenesis, Oncogene 28 (2009) 2545–2555.
[8] J. Rudolph, L.J. Murray, C.O. Ndubaku, T. O'Brien, E. Blackwood, W. Wang, I. Aliagas, L. Gazzard, J.J. Crawford, J. Drobnick, W. Lee, X. Zhao, K.P. Hoeflich, D.A. Favor, P. Dong, H. Zhang, C.E. Heise, A. Oh, C.C. Ong, H. La, P. Chakravarty, C. Chan, D. Jakubiak, J. Epler, S. Ramaswamy, R. Vega, G. Cain, D. Diaz, Y. Zhong, Chemically diverse group I p21-activated kinase (PAK) inhibitors impart acute cardiovascular toxicity with a narrow therapeutic window, J. Med. Chem. 59 (2016) 5520–5541.
[9] B.W. Murray, C. Guo, J. Piraino, J.K. Westwick, C. Zhang, J. Lamerdin, E. Dagostino, D. Knighton, C.M. Loi, M. Zager, E. Kraynov, I. Popoff, J.G. Christensen, R. Martinez, S.E. Kephart, J. Marakovits, S. Karlicek, S. Bergqvist, T. Smeal, Small-molecule p21-activated kinase inhibitor PF-3758309 is a potent inhibitor of oncogenic signaling and tumor growth, Proc. Nat. Acad. Sci. USA 107 (2010) 9446–9451.
[10] E.L. Bradshaw-Pierce, T.M. Pitts, A.C. Tan, K. McPhillips, M. West, D.L. Gustafson, C. Halsey, L. Nguyen, N.V. Lee, J.L. Kan, B.W. Murray, S.G. Eckhardt, Tumor P-glycoprotein correlates with efficacy of PF-3758309 in in vitro and in vivo models of colorectal cancer, Front. Pharmacol. 4 (2013) 1–11.
[11] O. Abu Aboud, C.H. Chen, W. Senapedis, E. Baloglu, C. Argueta, R.H. Weiss, Dual and specific inhibition of NAMPT and PAK4 By KPT-9274 decreases kidney cancer growth, Mol. Cancer Therap. 15 (2016) 2119–2129.
[12] W. Senapedis, Y. Landesman, M. Schenone, B. Karger, S. Wu, S. Shacham, E. Baloglu, Identification of novel small molecules as selective PAK4 allosteric modulators (PAMs) by stable isotope labeling of amino acids in cells (SILAC), Europ. J. Cancer 50 (2014) 156.
[13] C. Hao, X. Li, S. Song, B. Guo, J. Guo, J. Zhang, Q. Zhang, W. Huang, J. Wang, B. Lin, M. Cheng, F. Li, D. Zhao, Advances in the 1-phenanthryl-tetrahydroisoquinoline series of PAK4 inhibitors: potent agents restrain tumor cell growth and invasion, Org. Biomol. Chem. 14 (2016) 7676–7690.
[14] J. Guo, F. Zhao, W. Yin, M. Zhu, C. Hao, Y. Pang, T. Wu, J. Wang, D. Zhao, H. Li, M. Cheng, Design, synthesis, structure-activity relationships study and X-ray crystallography of 3-substituted-indolin-2-one-5-carboxamide derivatives as PAK4 inhibitors, Eur. J. Med. Chem. 155 (2018) 197–209.
[15] C. Hao, W. Huang, X. Li, J. Guo, M. Chen, Z. Yan, K. Wang, X. Jiang, S. Song, J. Wang, D. Zhao, F. Li, M. Cheng, Development of 2, 4-diaminoquinazoline derivatives as potent PAK4 inhibitors by the core refinement strategy, Eur. J. Med. Chem. 131 (2017) 1–13.
[16] J. Guo, M. Zhu, T. Wu, C. Hao, K. Wang, Z. Yan, W. Huang, J. Wang, D. Zhao, M. Cheng, Discovery of indolin-2-one derivatives as potent PAK4 inhibitors: Structure-activity relationship analysis, biological evaluation and molecular docking study, Bioorg. Med. Chem. 25 (2017) 3500–3511.
[17] J. Wang, M. Yan, D. Zhao, Y. Sha, F. Li, M. Cheng, Pharmacophore identification of PAK4 inhibitors, Mol. Simul. 36 (2010) 53–57.
[18] S. Song, X. Li, J. Guo, C. Hao, Y. Feng, B. Guo, T. Liu, Q. Zhang, Z. Zhang, R. Li, J. Wang, B. Lin, F. Li, D. Zhao, M. Cheng, Design, synthesis and biological evaluation of 1-phenanthryl-tetrahydroisoquinoline derivatives as novel p21-activated kinase 4 (PAK4) inhibitors, Org. Biomol. Chem. 13 (2015) 3803–3818.
[19] C. Hao, F. Zhao, H. Song, J. Guo, X. Li, X. Jiang, R. Huan, S. Song, Q. Zhang, R. Wang, K. Wang, Y. Pang, T. Liu, T. Lu, W. Huang, J. Wang, B. Lin, Z. He, H. Li, F. Li, D. Zhao, M. Cheng, Structure-based design of 6-chloro-4-aminoquinazoline-2-carboxamide derivatives as potent and selective p21-activated kinase 4 (PAK4) inhibitors, J. Med. Chem. 61 (2018) 265–285.
[20] J. Wang, G. Wang, Y. Sha, D.M. Zhao, F. Li, M.S. Cheng, Structure-based functional site recognition for p21-activated kinase 4, Arch. Pharm. Res. 36 (2013) 1494–1499.
[21] R. Li, X. Su, Z. Chen, W. Huang, Y. Wang, K. Wang, B. Lin, J. Wang, M. Cheng, Structure-based virtual screening and ADME/T-based profiling for low molecular weight chemical starting points as p21-activated kinase 4 inhibitors, RSC Adv. 5 (2015) 23202–23209.
[22] M. Kayikci, A.J. Venkatakrishnan, J. Scott-Brown, C.N.J. Ravarani, T. Flock, M.M. Babu, Visualization and analysis of non-covalent contacts using the Protein Contacts Atlas, Nat. Struct. Mol. Biol. 25 (2018) 185–194.
[23] J.J. Crawford, W. Lee, I. Aliagas, S. Mathieu, K.P. Hoeflich, W. Zhou, W. Wang, L. Rouge, L. Murray, H. La, N. Liu, P.W. Fan, J. Cheong, C.E. Heise, S. Ramaswamy, R. Mintzer, Y. Liu, Q. Chao, J. Rudolph, Structure-guided design of group I selective p21-activated kinase inhibitors, J. Med. Chem. 58 (2015) 5121–5136.
[24] Y. Zhou, J. Zhang, J. Wang, M.S. Cheng, D.M. Zhao, F. Li, Targeting PAK1 with the small molecule drug AK963/40708899 suppresses gastric cancer cell proliferation and invasion by downregulation of PAK1 activity and PAK1-related signaling pathways, Anat. Rec. (Hoboken) (2019).
[25] J.Z. Hong-Yan Zhang, Chen-Zhou Hao, Ying Zhou, Jian Wang, Mao-Sheng Cheng, Dong-Mei, F.L. Zhao, LC-0882 targets PAK4 and inhibits PAK4-related signaling pathways to suppress the proliferation and invasion of gastric cancer cells, Am. J. Trans. Res. 9 (6) (2017) 2736–2747.

[26] X. Li, Q. Ke, Y. Li, F. Liu, G. Zhu, F. Li, DGCR6L, a novel PAK4 interaction protein, regulates PAK4-mediated migration of human gastric cancer cell via LIMK1, Int. J. Biochem. Cell Biol. 42 (2010) 70–79.
[27] N. Gnesutta, J. Qu, A. Minden, The serine/threonine kinase PAK4 prevents caspase activation and protects cells from apoptosis, J. Biol. Chem. 276 (2001) 14414–14419.
[28] C.K. Rane, A. Minden, P21 activated kinase signaling in cancer, Semin. Cancer Biol. 6 (6) (2018) 459.
[29] N. Gnesutta, A. Minden, Death receptor-induced activation of initiator caspase 8 is antagonized by serine/threonine kinase PAK4, Mol. Cell Biol. 23 (2003) 7838–7848.
[30] X. Li, A. Minden, PAK4 functions in tumor necrosis factor (TNF) alpha-induced survival pathways by facilitating TRADD binding to the TNF receptor, J. Biol. Chem. 280 (2005) 41192–41200.
[31] N. Yang, O. Higuchi, K. Ohashi, K. Nagata, A. Wada, K. Kangawa, E. Nishida, K. Mizuno, Cofilin phosphorylation by LIM-kinase 1 and its role in Rac-mediated actin reorganization, Nature 393 (1998) 809.
[32] Q. Guo, N. Su, J. Zhang, X. Li, Z. Miao, G. Wang, M. Cheng, H. Xu, L. Cao, F. Li, PAK4 kinase-mediated SCG10 phosphorylation involved in gastric cancer metastasis, Oncogene 33 (2014) 3277–3287.
[33] M. Wilchek, E.A. Bayer, The avidin-biotin complex in immunology, Immunol. Today 5 (1984) 39–43.
[34] M. Wilchek, E.A. Bayer, The avidin-biotin complex in bioanalytical applications, Anal. Biochem. 171 (1988) 1–32.
[35] Y. Wang, B. Hu, Y. Peng, X. Xiong, W. Jing, J. Wang, H.-Y. Gao, In silico exploration of the molecular mechanism of cassane diterpenoids on anti-inflammatory and immunomodulatory activity, J. Chem. Inform. Model. (2019).